

Nanotheranostics and Image-Guided Drug Delivery: Current Concepts and Future Directions

Twan Lammers,^{*,†,‡,§} Fabian Kiessling,[‡] Wim E. Hennink,[†] and Gert Storm[†]

Department of Pharmaceutics, Utrecht Institute for Pharmaceutical Sciences, Utrecht University, Sorbonnelaan 16, 3584 CA Utrecht, The Netherlands, Department of Experimental Molecular Imaging, RWTH–Aachen University, Pauwelsstrasse 30, 52074 Aachen, Germany, and Department of Innovative Cancer Diagnosis and Therapy, Clinical Cooperation Unit Radiotherapeutic Oncology, German Cancer Research Center, 69120 Heidelberg, Germany

Received July 7, 2010; Revised Manuscript Received August 31, 2010; Accepted September 7, 2010

Abstract: Nanomedicine formulations aim to improve the biodistribution and the target site accumulation of systemically applied (chemo-) therapeutics. Various different passively and actively targeted nanomedicines have been evaluated over the years, based e.g. on liposomes, polymers, micelles and antibodies, and a significant amount of (pre-) clinical evidence has been obtained showing that these 5–200 nm sized carrier materials are able to improve the therapeutic index of low-molecular-weight drugs. Besides for therapeutic purposes, however, nanomedicine formulations have also been more and more used for imaging applications, as well as, in recent years, for theranostic approaches, i.e. for systems and strategies in which disease diagnosis and therapy are combined. Potential applications of theranostic nanomedicine formulations range from the noninvasive assessment of the biodistribution and the target site accumulation of low-molecular-weight drugs, and the visualization of drug distribution and drug release at the target site, to the optimization of strategies relying on triggered drug release, and the prediction and real-time monitoring of therapeutic responses. Nanotheranostic systems are consequently considered to be highly suitable systems for (pre-) clinical implementation, not only because they might assist in better understanding various important aspects of the drug delivery process, and in developing better drug delivery systems, but also because they might contribute to realizing the potential of “personalized medicine”, and to developing more effective and less toxic treatment regimens for individual patients.

Keywords: Nanomedicines; theranostics; theragnostics; image-guided drug delivery; drug targeting; molecular imaging; liposomes; polymers; micelles; antibodies

Introduction

Many routinely used (chemo-) therapeutic agents suffer from poor pharmacokinetics and from an inappropriate biodistribution. Because of their low molecular weight, for instance, intravenously administered (anticancer) drugs are

generally rapidly cleared from the circulation, and they do not accumulate well at the pathological site. In addition to this, because of their small size and/or their high hydrophobicity, (chemo-) therapeutic drugs tend to present with a large volume of distribution, and they accumulate in and cause toxicity toward various different healthy tissues. Consequently, many agents which have been shown to be highly effective *in vitro* often not only are relatively ineffective when administered *in vivo* but also tend to be relatively toxic.

To assist *iv* applied (chemo-) therapeutic agents in achieving proper pharmacokinetics and an appropriate target site accumulation, and to thereby improve the balance

* Corresponding author. Mailing address: Utrecht University, Department of Pharmaceutics, Sorbonnelaan 16, 3584 CA Utrecht, The Netherlands. E-mail: t.lammers@uu.nl; tlammers@ukaachen.de. Tel: 0031-302537304. Fax: 0031-302517839.

† Utrecht University.

‡ RWTH–Aachen University.

§ German Cancer Research Center.

between their efficacy and their toxicity, a large number of drug delivery systems have been designed and evaluated over the years.^{1–5} Clinically relevant examples of such nanometer-sized carrier materials are liposomes, polymers, micelles and antibodies. The former three nanomedicine systems generally primarily aim to improve the circulation time of the conjugated or entrapped (chemo-) therapeutic agent, and to improve its accumulation at the pathological site by means of enhanced permeability and retention (EPR) mediated passive drug targeting.^{6,7} The latter, on the other hand, i.e. antibody-based carrier materials, are primarily designed to improve target cell recognition and target cell uptake, and to improve the efficacy of the attached active agent by means of active drug targeting.

Passively and actively targeted nanomedicine formulations have been used to treat various different diseases. PEGylated proteins, for instance, have been approved for improving the treatment of hepatitis (PegIntron and PegAsys), of acromegaly (PegVisomant) and of severe combined immunodeficiency (SCID; Adagen).⁸ Liposomal nanomedicines are for example routinely implemented in the management of fungal infections (AmBisome) and of lymphomatous meningitis (DepoCyt).⁹ By far the most progress in this regard, however, has been made in the field of oncology. Two different liposomal doxorubicin formulations, i.e. Myocet (unPEGylated) and Doxil (PEGylated; Caelyx in Europe), are for instance being used to treat Kaposi sarcoma, multiple myeloma, metastatic breast cancer and ovarian carcinoma, and liposomal vincristine (Onco-TCS) to treat non-Hodgkin's lymphoma.¹⁰ PEGylated L-asparaginase (Oncaspar) and poly(styrene-co-maleic acid)-modified neocarzinostatin (SMANCS) have been implemented in the treatment of acute lymphoblastic leukemia hepatocellular carcinoma, respec-

tively, and albumin- and poly(L-glutamic acid)-based paclitaxel (i.e., Abraxane and Xyotax) in the management of breast and non-small cell lung cancer.¹¹ Examples of antibody-based actively targeted nanomedicines approved for clinical use are Zevalin (yttrium-90-labeled ibritumomab-tiuxetan) and Ontak (denileukin diftitox), which are used for non-Hodgkin's lymphoma and cutaneous T-cell lymphoma, respectively.¹² Many other passively and actively targeted nanomedicines are currently being evaluated in (pre-) clinical trials, and it is expected that, in the next five to ten years, several additional nanomedicine formulations will gain FDA and/or EMEA approval.

Besides for therapeutic applications, passively and actively targeted nanomedicines are also more and more being used for diagnostic purposes. Antibodies, liposomes, polymers and micelles carrying contrast agents, such as radionuclides and MR imaging probes, have for instance on several occasions already been shown to hold potential for detecting diseases, as well as for visualizing various important aspects of the drug delivery process. In addition to this, more and more nanomedicine formulations are being prepared in which diagnostic and therapeutic agents are combined. To this end, on the one hand, "classic" drug targeting systems, such as antibodies, liposomes, polymers and micelles, are being cofunctionalized both with contrast agents and with drugs. On the other hand, also nanomaterials with an intrinsic ability to be used for imaging purposes, such as iron oxides and quantum dots, are increasingly implemented for combining disease diagnosis and therapy. Ever more of such theranostic nanomedicine materials have been designed and evaluated over the past few years, and ever more interesting applications have been envisioned for nanotheranostics. As will be outlined below, and as depicted schematically in Figure 1, nanotheranostics can be used to noninvasively assess the biodistribution and the target site accumulation of coconjugated or coentrapped (chemo-) therapeutic agents, to monitor and quantify drug release, to facilitate therapeutic interventions relying on triggered drug release, to predict therapeutic responses, and to longitudinally monitor the efficacy of therapeutic interventions.

- (1) Torchilin, V. P. Drug targeting. *Eur. J. Pharm. Sci.* **2000**, *11*, S81–S91.
- (2) Allen, T. M.; Cullis, P. R. Drug delivery systems: entering the mainstream. *Science* **2004**, *303*, 1818–1822.
- (3) Peer, D.; Karp, J. M.; Hong, S.; Farokhzad, O.; Margalit, R.; Langer, R. Nanocarriers as an emerging platform for cancer therapy. *Nat. Nanotechnol.* **2007**, *2*, 751–760.
- (4) Davis, M. E.; Chen, Z. G.; Shin, D. M. Nanoparticle therapeutics: an emerging treatment modality for cancer. *Nat. Rev. Drug Discovery* **2008**, *7*, 771–782.
- (5) Lammers, T.; Hennink, W. E.; Storm, G. Tumour-targeted nanomedicines: principles and practice. *Br. J. Cancer* **2008**, *99*, 392–397.
- (6) Maeda, H.; Matsumura, Y. A new concept for macromolecular therapeutics in cancer chemotherapy: mechanism of tumorotropic accumulation of proteins and the antitumor agent Smancs. *Cancer Res.* **1986**, *46*, 6387–6392.
- (7) Maeda, H.; Wu, J.; Sawa, T.; Matsumura, Y.; Hori, K. Tumour vascular permeability and the EPR effect in macromolecular therapeutics: a review. *J. Controlled Release* **2000**, *65*, 271–284.
- (8) Duncan, R. The dawning era of polymer therapeutics. *Nat. Rev. Drug Discovery* **2003**, *2*, 347–360.
- (9) Torchilin, V. P. Recent advances with liposomes as pharmaceutical carriers. *Nat. Rev. Drug Discovery* **2005**, *4*, 145–160.
- (10) Hofheinz, R. D.; Gnäd-Vogt, S. U.; Beyer, U.; Hochhaus, A. Liposomal encapsulated anti-cancer drugs. *Anticancer Drugs* **2005**, *16*, 691–707.

1. Visualizing Biodistribution in Real Time. Nanomedicine formulations are designed to improve the biodistribution and the target site accumulation of systemically applied (chemo-) therapeutic agents. To facilitate biodistributional analyses, it would be advantageous if the circulation time and the organ accumulation of nanomedicine systems—or, even better, of the conjugated or entrapped (chemo-) therapeutic drug—could be visualized noninvasively *in vivo* in real time. To achieve this goal, many different nanomedicines have, besides with drugs, been cofunctionalized with contrast agents, in order to track their pharmacokinetics and their biodistribution.

- (11) Duncan, R. Polymer conjugates as anticancer nanomedicines. *Nat. Rev. Cancer* **2006**, *6*, 688–701.
- (12) Allen, T. M. Ligand-targeted therapeutics in anticancer therapy. *Nat. Rev. Cancer* **2002**, *2*, 750–763.

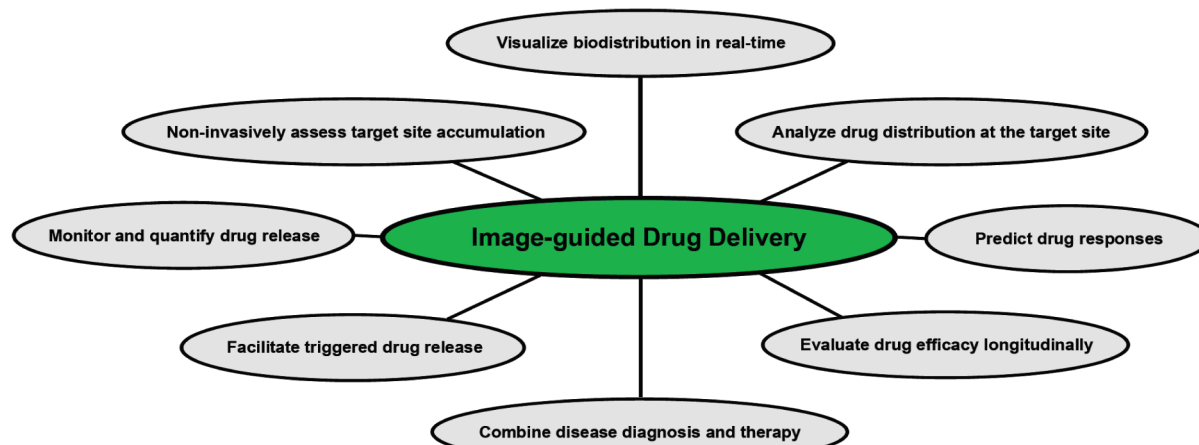


Figure 1. Nanotheranostics and image-guided drug delivery. Schematic representation of applications of nanotheranostics and image-guided drug delivery. By coinorporating pharmacologically active agents and contrast agents in a single nanomedicine formulation, it is possible to predict and improve the outcome of the intervention, and to visualize and better understand various important aspects of the drug delivery process. Reproduced with permission from ref 36. Copyright 2010 Elsevier Ltd. See text for details.

In the majority of cases, radionuclides have been used for this purpose. Several different types of radionuclide-labeled antibodies, liposomes, polymers and micelles have been subjected to biodistributional analyses over the years, both in animal models and in patients, and it has become clear that such studies substantially assist in improving our understanding of the drug delivery process, as well as in predicting the therapeutic potential of (tumor-) targeted nanomedicines. Figure 2A–D in regard shows the biodistribution of indium-111-labeled PEGylated liposomes at 72 h after iv injection into a patient suffering from squamous cell carcinoma, exemplifying by means of single photon emission computed tomography (SPECT) that, at this time point, a substantial amount of the passively tumor-targeted nanomedicine formulation is still present in systemic circulation (i.e., in the cardiac blood pool (CP)), while a significant portion has also already localized to the target site (i.e., to a tumor mass situated at the tongue base (Tu)).¹³ The remainder of the radiolabeled liposomes was found in organs of the reticuloendothelial system (i.e., RES; like liver (L) and spleen (Spl)), which are known to be involved in the clearance of long-circulating nanomedicines.

In comparable analyses, Seymour and colleagues showed by means of γ -scintigraphy that an iodine-123-labeled

galactosamine-containing (i.e., hepatocyte-targeted) polymeric prodrug of doxorubicin effectively localized to the liver (Figure 2E), whereas a comparable formulation lacking galactosamine failed to show liver localization (Figure 2F).¹⁴ Interestingly, however, the latter, i.e. the galactosamine-free passively tumor-targeted polymeric prodrug, did localize relatively effectively to tumors by means of EPR, as exemplified by the fact that significant retention was observed in the shoulder region of a patient suffering from a large clavicular metastasis (Figure 1G).

Similarly, also in a large number of animal experiments, radionuclide-labeled antibodies, liposomes, polymers and micelles have been shown to be highly useful for monitoring the biodistribution of nanomedicine-associated therapeutic agents. As exemplified by Figure 2H–J, for instance, upon labeling three differently sized HPMA (i.e., *N*-(2-hydroxypropyl)methacrylamide)) copolymers with iodine-131, a clear correlation between their size (i.e., their average molecular weight) and their circulation time and tumor accumulation could be observed: at 24 h post iv injection (p.i.), 24%, 11% and 6% of the injected dose were still present in blood for the 65 kDa, the 31 kDa and the 23 kDa copolymer, respectively, as compared to less than 0.0001% for the free label (Figure 2H).¹⁵ In line with this, and in line with the principles of EPR-mediated passive drug targeting, at 24, 72, and 168 h p.i., significantly higher levels of the higher molecular weight copolymers were detected in tumors (Figure 2I,J). Together, these insights and efforts exemplify that the cofunctionalization of nanomedicine formulations both with drugs and with contrast agents enables a noninvasive assessment of their biodistribution, and they thereby emphasize that such theranostic approaches are highly suitable for evaluating the *in vivo* potential of (tumor-) targeted nanomedicines.

- (13) Harrington, K. J.; Mohammadtaghi, S.; Uster, P. S.; Glass, D.; Peters, A. M.; Vile, R. G.; Stewart, J. S. Effective targeting of solid tumors in patients with locally advanced cancers by radiolabeled pegylated liposomes. *Clin. Cancer Res.* **2001**, *7*, 243–254.
- (14) Seymour, L. W.; Ferry, D. R.; Anderson, D.; Hesslewood, S.; Julyan, P. J.; Poyner, R.; Doran, J.; Young, A. M.; Burles, S.; Kerr, D. J. Hepatic drug targeting: phase I evaluation of polymer-bound doxorubicin. *J. Clin. Oncol.* **2002**, *20*, 1668–1676.
- (15) Lammers, T.; Kühlein, R.; Kissel, M.; Subr, V.; Etrych, T.; Pola, R.; Pechar, M.; Ulbrich, K.; Storm, G.; Huber, P.; Peschke, P. Effect of physicochemical modification on the biodistribution and tumor accumulation of HPMA copolymers. *J. Controlled Release* **2005**, *110*, 103–118.

2. Noninvasively Assessing Target Site Accumulation. In addition to monitoring the biodistribution of nanomedicine formulations in real time, nanotheranostics can also be used

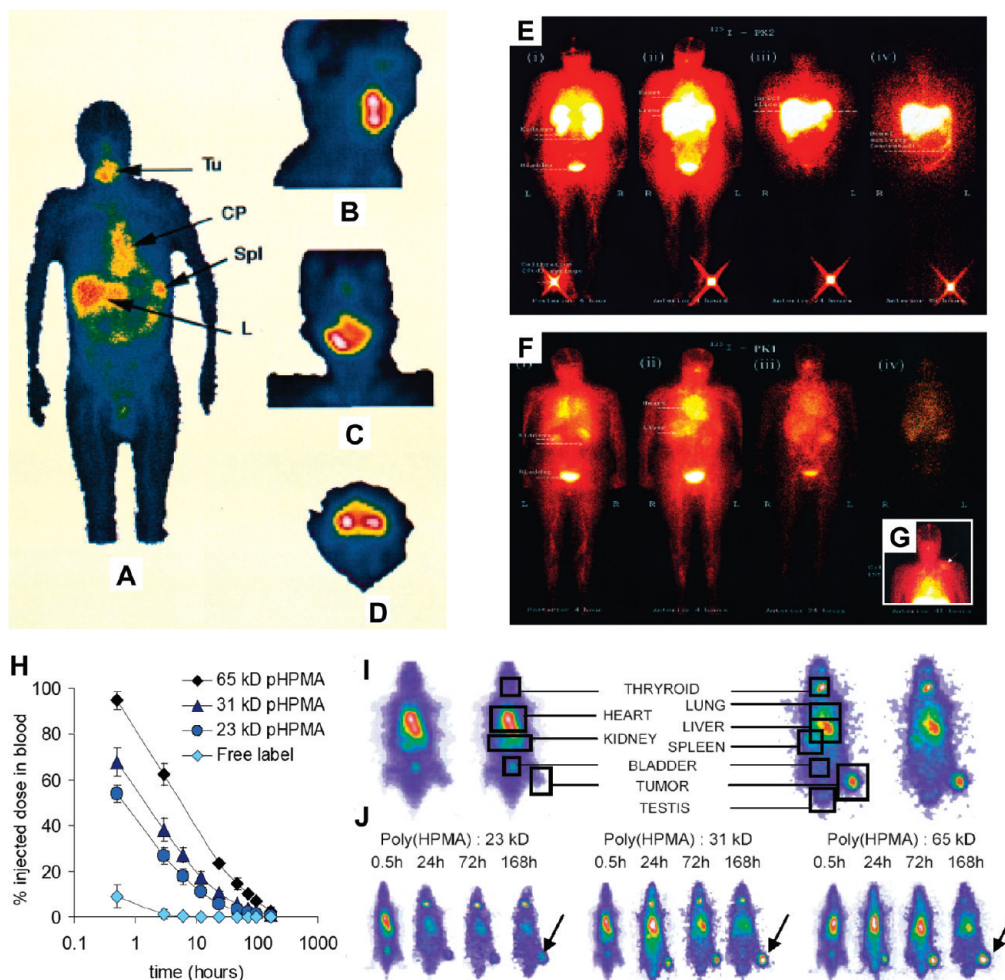


Figure 2. Nanotheranostics for visualizing biodistribution in real-time. A–D: Gamma-camera images of a patient suffering from a squamous cell carcinoma at the tongue base, obtained at 72 h after the iv injection of ^{111}In -labeled PEGylated liposomes. The whole body scan in A reveals accumulation in tumor (Tu), cardiac blood pool (CP), liver (L) and spleen (Spl). A certain degree of accumulation in the bowel can also be observed. The sagittal (B), coronal (C) and transverse (D) SPECT images confirm accumulation at the pathological site. Adapted and reprinted with permission from ref 13. Copyright 2001 American Association for Cancer Research. E–G: Planar gamma-camera imaging of patients treated with galactosamine-modified liver-targeted pHPMA-GFLG-doxorubicin (i.e., ^{131}I -labeled PK2; E) and with nonmodified passively targeted pHPMA-GFLG-doxorubicin (i.e., ^{131}I -labeled PK1; F, G) at 4 (i and ii), 24 (iii) and 48 (iv) hours after iv administration. In G, the accumulation of the passively tumor-targeted polymeric prodrug in a large clavicular metastasis can be observed. In such whole body analyses, calibration is generally performed using an external standard, placed adjacent to the patients' feet (as in E), in order to quantify the biodistribution of the agents. Reproduced with permission from ref 14. Copyright 2002 American Society for Clinical Oncology. H–J: Analysis of the pharmacokinetics, the biodistribution and the tumor accumulation of three differently sized ^{131}I -labeled HPMA copolymers in Copenhagen rates bearing subcutaneously transplanted Dunning AT1 tumors, exemplifying prolonged circulation times (H) and effective and selective tumor localization (J). Reproduced with permission from ref 15. Copyright 2005 Elsevier B.V.

to noninvasively assess target site accumulation. Both radionuclide- and MR contrast agent-labeled nanomedicines are highly suitable for monitoring the targeted drug delivery to the pathological sites. As exemplified by Figure 3A,B, for instance, indium-111-labeled Zevalin effectively accumulates in an abdominal tumor in a non-Hodgkin's lymphoma (NHL) patient.¹⁶ Zevalin is a CD20-directed radiotherapeutic antibody which is administered to patients

with follicular NHL who have achieved a partial response to first-line chemotherapy, as well as to patients with relapsed or refractory low-grade follicular B-cell NHL. The SPECT and the corresponding anatomical computed tomography (CT) images in Figure 3A,B clearly show that the antibody effectively localizes to the target site over time, thereby providing important information with regard to the potential efficacy of the intervention.

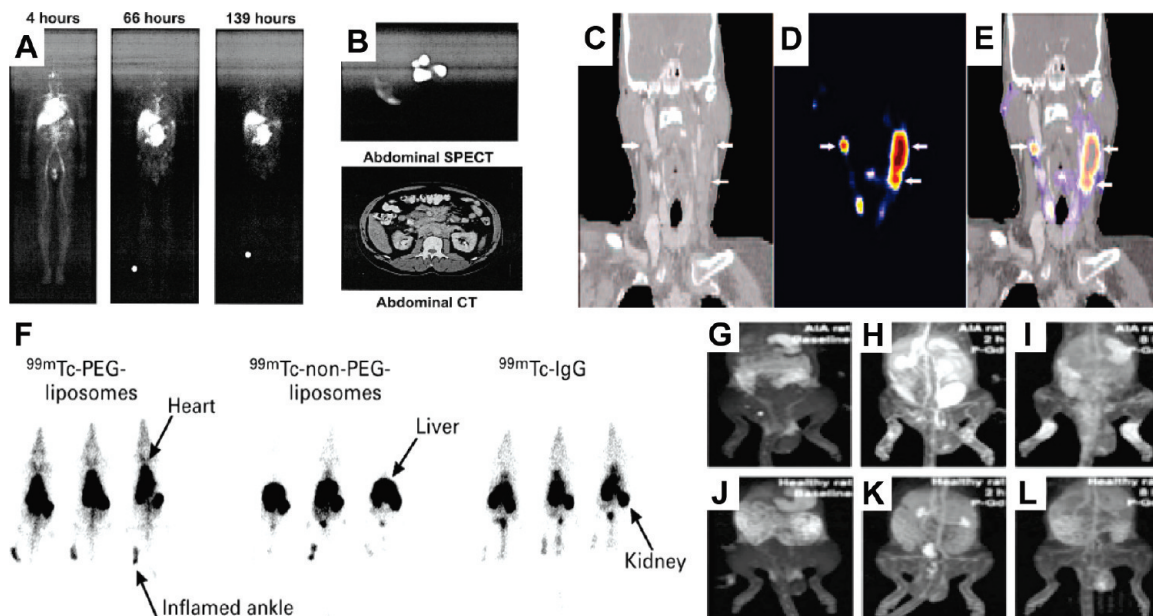


Figure 3. Nanotheranostics for noninvasively assessing target site accumulation. A: Serial anterior whole body gamma-camera images obtained in a patient with a bulky abdominal tumor mass, demonstrating effective target site accumulation of ¹¹¹In-labeled Zevalin. B: Abdominal SPECT (for visualizing target site accumulation) and CT (for visualizing anatomy) images, correlating Zevalin uptake with abdominal adenopathy. Reproduced with permission from ref 16. Copyright 2001 Elsevier Science Ireland Ltd. C–E: Fusion (E) of computed tomography (C) and coronal immunopositron emission tomography (D) images upon the iv injection of the ⁸⁹Zr-labeled monoclonal antibody U36 into a head and neck cancer patient with a tumor in the left tonsil and with lymph node metastases at the left and right side of the neck (arrows). Images were obtained at 72 h after iv injection. Reproduced with permission from ref 17. Copyright 2007 AlphaMed Press. F: Scintigraphic analysis of rats with adjuvant arthritis imaged 24 h after iv injection of ^{99m}Tc-labeled PEGylated liposomes, non-PEGylated liposomes and IgG. Three representative animals are shown for each experimental group. Reproduced with permission from ref 18. Copyright 1997 BMJ Publishing Group. G–L: Maximum intensity projection MR images of adjuvant-induced arthritic (G–I) and healthy (J–L) rats at baseline (G and J), and at 2 (H and K) and 8 (I and L) h after the iv injection of a gadolinium-labeled HPMA copolymer. Reproduced with permission from ref 22. Copyright 2004 Springer Science+Business Media, Inc.

Analogously, also an experimental zirconium-89-labeled monoclonal antibody, i.e. U36, was shown to be able to effectively accumulate at the pathological site.¹⁷ In this case, as shown in Figure 3C–E, the zirconium-based positron emission tomography (PET) signals associated with the antibody clearly colocalized with the CT-visualized tumorous tissue in the tonsils and in the lymph nodes of a head and neck cancer patient.

In an animal model of rheumatoid arthritis, comparable observations were made using technetium-99m-labeled PEGylated liposomes. Like tumors, also severely inflamed arthritic joints are characterized by an enhanced vascular leakiness, enabling long-circulating nanomedicines to extravasate into these lesions by means of EPR. Figure 3F exemplifies in this regard that PEGylated liposomes, which circulate substantially longer than unPEGylated liposomes and IgG, accumulated in the inflamed joints of rats suffering from adjuvant arthritis significantly more efficiently than did the other two carrier materials.¹⁸ As a result of this effective target site localization, in subsequent studies, PEGylated liposomes containing the corticosteroid prednisolone phosphate were found to be highly effective in inhibiting both adjuvant and collagen-induced arthritis.^{28–30} Clinical studies

with this long-circulating liposomal corticosteroid formulation, termed NanoCort, are currently ongoing.

Similar findings have recently been reported by Wang and colleagues, who instead of PEGylated liposomes used HPMA copolymers as long-circulating and passively disease site-targeted nanocarriers. To provide proof-of-principle for target site accumulation, they developed a theranostic nanomedicine formulation containing gadolinium, and they demonstrated by means of magnetic resonance imaging (MRI) that Gd-DO3A-modified poly(HPMA) effectively accumulates in the ankles of rats suffering from adjuvant-induced arthritis, whereas no accumulation was observed in the ankles of healthy rats (Figure 3G–L).²² In line with this, and in line with the above results on the efficacy of liposomal prednisolone phosphate, follow-up experiments showed that conjugating the corticosteroid drug dexamethasone to a long-circulating HPMA copolymer yielded a substantial improvement in disease inhibition,^{23–25} indicating that also this passively targeted anti-inflammatory nanomedicine formulation might hold significant clinical potential.

3. Monitoring Drug Distribution at the Target Site. Besides studying the overall levels of drug accumulation at the target site, it is also important to visualize and analyze

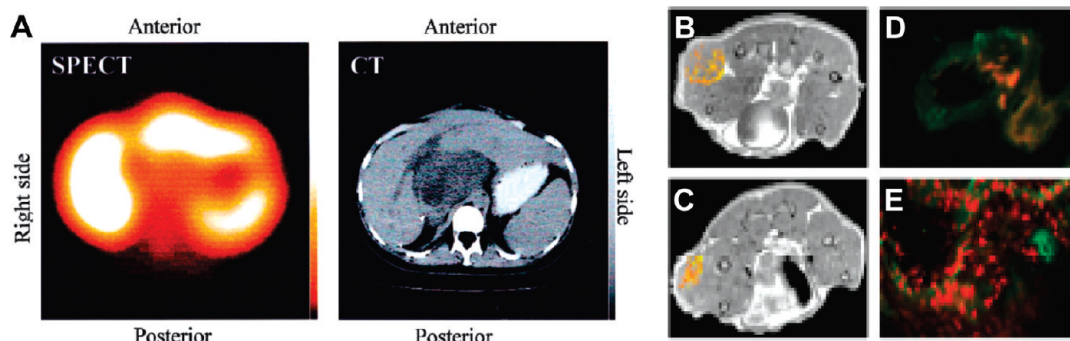


Figure 4. Nanotheranostics for monitoring drug distribution at the target site. A: SPECT and CT images obtained in a patient with liver cancer upon the iv administration of ^{123}I -labeled PK2 (i.e., galactosamine-modified and liver-targeted pHMPA-GFLG-doxorubicin). Image analysis of radioactivity distribution at the target site enabled the quantification of the efficacy of hepatic drug targeting ($16.9 \pm 3.9\%$ of the injected dose). Furthermore, image coregistration, i.e. superimposition of the biodistributional SPECT scan and the anatomical CT scan, revealed that the majority of the radiolabeled polymeric prodrug accumulated in the healthy (peripheral) parts of the liver, and that only relatively low levels localized in the tumorous region (i.e., in the “dark” center of the CT image; $3.3 \pm 5.6\%$ ID). Images reproduced with permission from ref 14. Copyright 2002 American Society for Clinical Oncology. B, C: MR images of subcutaneous tumors in mice after the iv injection of gadolinium-labeled RGD-targeted liposomes (which specifically bind to $\alpha\beta 3$ integrins expressed on angiogenic blood vessels; B) and of gadolinium-labeled control liposomes (i.e., RAD-targeted; C). D, E: Fluorescence microscopy analyses confirming the specific binding of RGD-targeted gadolinium- and rhodamine-containing liposomes to tumor blood vessels. Red fluorescence represents liposomes and green fluorescence represents blood vessels (CD31 staining). RGD-targeted liposomes were exclusively found within the vessel lumen or associated with tumor endothelial cells (D), whereas RAD-modified liposomes were also found outside blood vessels, i.e. in the interstitium of the tumor (E). Images reproduced with permission from ref 26. Copyright 2005 FASEB.

drug distribution at the target site, not only to more extensively and more detailedly evaluate the spatial parameters of targeted drug delivery but also to better understand and better predict why certain treatments are effective, and others are not. In the above-mentioned study focusing on galactosamine-modified HPMA copolymer-bound doxorubicin (i.e., PK2), for instance, in which the incorporation of the sugar-based targeting moiety galactosamine was shown to be highly effective in inducing liver uptake, it was also found that only a relatively low level of the total amount of copolymer accumulating in the liver actually localized to tumorous tissue.¹⁴ This was observed upon superimposing anatomical CT and functional SPECT images, which highlighted that most of the polymer-associated radioactivity could be attributed to healthy liver ($16.9 \pm 3.9\%$ ID), and that only a small fraction—which was nonetheless substantially above background—accumulated in liver tumors ($3.3 \pm 5.6\%$ ID; Figure 4A). This somewhat disappointing observation can be explained by taking the smaller size of liver tumors compared to healthy livers into account, as well as the fact that liver tumors tend to be less well-perfused and less well-vascularized. This notion underlines the importance of monitoring and quantifying drug distribution at the target site, and it exemplifies that multiple imaging modalities, providing besides anatomical information also functional and/or molecular feedback, are needed to meaningfully predict the efficacy of targeted therapeutic interventions.

Comparable efforts with regard to visualizing drug distribution at the target site have been undertaken using

gadolinium-labeled liposomes. Mulder, Nicolay and colleagues, for instance, have recently shown in this regard that RGD-modified endothelial cell-targeted liposomes and RAD-modified control liposomes distribute quite differently within tumors.^{26,27} As exemplified by Figure 4B–E, it was found that liposomes targeted to endothelial cells accumulated much more strongly in the angiogenic rim of subcutaneously transplanted B16 tumors, whereas control liposomes distributed much more evenly within these tumors (Figure 4B,D). This finding could be confirmed using immunohistochemistry

- (16) Wiseman, G. A.; White, C. A.; Sparks, R. B.; Erwin, W. D.; Podoloff, D. A.; Lamonica, D.; Bartlett, N. L.; Parker, J. A.; Dunn, W. L.; Spies, S. M.; Belanger, R.; Witzig, T. E.; Leigh, B. R. Biodistribution and dosimetry results from a phase III prospectively randomized controlled trial of Zevalin radioimmunotherapy for low-grade, follicular, or transformed B-cell non-Hodgkin’s lymphoma. *Crit. Rev. Oncol. Hematol.* **2001**, *39*, 181–194.
- (17) Van Dongen, G. A. M. S.; Visser, G. W. M.; Lub-De Hooghe, M. N.; De Vries, E. G.; Perk, L. R. Immuno-PET: A navigator in monoclonal antibody development and applications. *Oncologist* **2007**, *12*, 1379–1389.
- (18) Boerman, O. C.; Oyen, W. J.; Storm, G.; Corvo, M. L.; van Bloois, L.; van der Meer, J. W.; Corstens, F. H. Technetium-99m labelled liposomes to image experimental arthritis. *Ann. Rheum. Dis.* **1997**, *56*, 369–373.
- (19) Metselaar, J. M.; van den Berg, W. B.; Holthuysen, A. E.; Wauben, M. H.; Storm, G.; van Lent, P. L. Liposomal targeting of glucocorticoids to synovial lining cells strongly increases therapeutic benefit in collagen type II arthritis. *Ann. Rheum. Dis.* **2004**, *63*, 348–353.

(Figure 4C,E), thereby suggesting that image-guided nanotheranostic systems are highly suitable systems for noninvasively assessing drug distribution at the target site.

4. Visualizing Drug Release. Another interesting application of nanotheranostics and image-guided drug delivery relates to the possibility of using these systems for visualizing drug release. As the vast majority of therapeutic agents used in nanomedicine formulations are inactive when conjugated to or entrapped in the carrier material, it is important to ensure that the agents are actually being released. *In vitro*, this can generally be done relatively easily, e.g. using HPLC, but *in vivo*, confirming drug release is much more complicated. After harvesting the target organ or tissue, for instance, the material generally needs to be homogenized, and the cells need to be lysed, in order to release the agents from certain intracellular compartments. During these processing steps, and especially during cell lysis (which is generally performed using detergents), many types of carrier materials are also destabilized, and e.g. in the case of liposomes, it then is impossible to discriminate between the amount of active agent that was still present within the liposomes at the point of harvesting and homogenization, and the amount that was already released into the extra- and intracellular environment.

- (20) Metselaar, J. M.; Wauben, M. H.; Wagenaar-Hilbers, J. P.; Boerman, O. C.; Storm, G. Complete remission of experimental arthritis by joint targeting of glucocorticoids with long-circulating liposomes. *Arthritis Rheum.* **2003**, *48*, 2059–2066.
- (21) Metselaar, J. M.; Wauben, M. H.; Wagenaar-Hilbers, J. P.; Boerman, O. C.; Storm, G. Liposomes in the treatment of inflammatory disorders. *Expert Opin. Drug Delivery* **2005**, *2*, 465–476.
- (22) Wang, D.; Miller, S. C.; Sima, M.; Parker, D.; Buswell, H.; Goodrich, K. C.; Kopeckova, P.; Kopecek, J. The arthrotropism of macromolecules in adjuvant-induced arthritis rat model: a preliminary study. *Pharm. Res.* **2004**, *21*, 1741–1749.
- (23) Wang, D.; Miller, S. C.; Liu, X. M.; Anderson, B.; Wang, X. S.; Goldring, S. R. Novel dexamethasone-HPMA copolymer conjugate and its potential application in treatment of rheumatoid arthritis. *Arthritis Res. Ther.* **2007**, *9*, R2.
- (24) Liu, X. M.; Quan, L. D.; Tian, J.; Alnouti, Y.; Fu, K.; Thiele, G. M.; Wang, D. Synthesis and evaluation of a well-defined HPMA copolymer-dexamethasone conjugate for effective treatment of rheumatoid arthritis. *Pharm. Res.* **2008**, *25*, 2910–2919.
- (25) Liu, X. M.; Miller, S. C.; Wang, D. Beyond oncology - application of HPMA copolymers in non-cancerous diseases. *Adv. Drug Delivery Rev.* **2010**, *62*, 258–271.
- (26) Mulder, W. J.; Strijkers, G. J.; Habets, J. W.; Bleeker, E. J.; van der Schaft, D. W.; Storm, G.; Koning, G. A.; Griffioen, A. W.; Nicolay, K. MR molecular imaging and fluorescence microscopy for identification of activated tumor endothelium using a bimodal lipidic nanoparticle. *FASEB J.* **2005**, *19*, 2008–2010.
- (27) Mulder, W. J.; Strijkers, G. J.; van Tilborg, G. A.; Griffioen, A. W.; Nicolay, K. Lipid-based nanoparticles for contrast-enhanced MRI and molecular imaging. *NMR Biomed.* **2006**, *19*, 142–164.
- (28) Viglianti, B. L.; Abraham, S. A.; Michelich, C. R.; Yarmolenko, P. S.; MacFall, J. R.; Bally, M. B.; Dewhirst, M. W. *In vivo* monitoring of tissue pharmacokinetics of liposome/drug using MRI: illustration of targeted delivery. *Magn. Reson. Med.* **2004**, *51*, 1153–1162.

To overcome this shortcoming, and to enable noninvasive analyses on (the kinetics of) drug release *in vivo*, nanotheranostics have been developed in which drugs and imaging agents are coin incorporated into the same delivery system. Since radionuclides render similar signals both in bound/trapped and in unbound/free form, these imaging agents are not suitable for visualizing drug release. MR contrast agents, on the other hand, such as gadolinium and manganese, depend on the interaction with surrounding water molecules to generate a signal, and since this interaction varies substantially when these agents are present within vs outside of water-impermeable vesicles, such as liposomes, MR probes are highly suitable for monitoring drug release.

A highly elegant approach in this regard has been published by Dewhirst and colleagues, who have used manganese sulfate ($MnSO_4$) both to load doxorubicin into liposomes (by means of a method comparable to that used in ammonium sulfate/pH gradient loading) and to generate a significant increase in MR signal upon drug and contrast agent release.^{28–30} Standard (nonthermosensitive; NTSL) and temperature-sensitive liposomes (TSL) were used in these studies, which included both *in vitro* and *in vivo* experiments, and it was shown that the relaxivity—i.e. the potential for MR signal enhancement—of TSL at temperatures below the transition temperature (T_g) was comparable to that of NTSL, but that it substantially increased upon heating to temperatures exceeding the T_g (i.e., $> 39.5^\circ\text{C}$), indicating release of Mn^{2+} from the liposomes.²⁸ These findings were confirmed in two follow-up analyses, in which contrast agent release from TSL was correlated with doxorubicin release, and in which drug dose painting was performed on the basis of MRI. Regarding the former, as demonstrated in Figure 5A–F, TSL rapidly released their contents upon iv administration to rats bearing preheated fibrosarcoma tumors, and they primarily did so in the well-vascularized and well-perfused periphery of the tumors.²⁹ Figure 5G–I shows that contrast agent release, which was determined noninvasively by means of MRI, correlated well with doxorubicin release, which was analyzed invasively using HPLC and fluorescence. Regarding drug dose painting, as exemplified by Figure 5J,K, clear-cut differences in drug and contrast agent release were observed when different heating protocols were implemented.³⁰ When the $MnSO_4$ and doxorubicin coloaded TSL were—as in the above example— injected into rats during steady-state hyperthermia, i.e. at a time point when the tumors were already homogeneously heated, then release was mainly observed in the periphery, where the large arteries are (Figure 5J). In this case, the vast majority of drug and contrast agent was apparently already released before the TSL could penetrate into the central regions of the tumor. Rats injected with TSL before the initiation of hyperthermia, on the other hand, displayed a release and signal enhancement pattern that followed the initial wave of heat as it emanated from the hyperthermia-generating catheter in the middle of the tumor (i.e., at the cross-section of the lines in panel J), resulting in a central enhancement (Figure 5K). In this case, injection of the liposomes before hyperthermia apparently enabled the

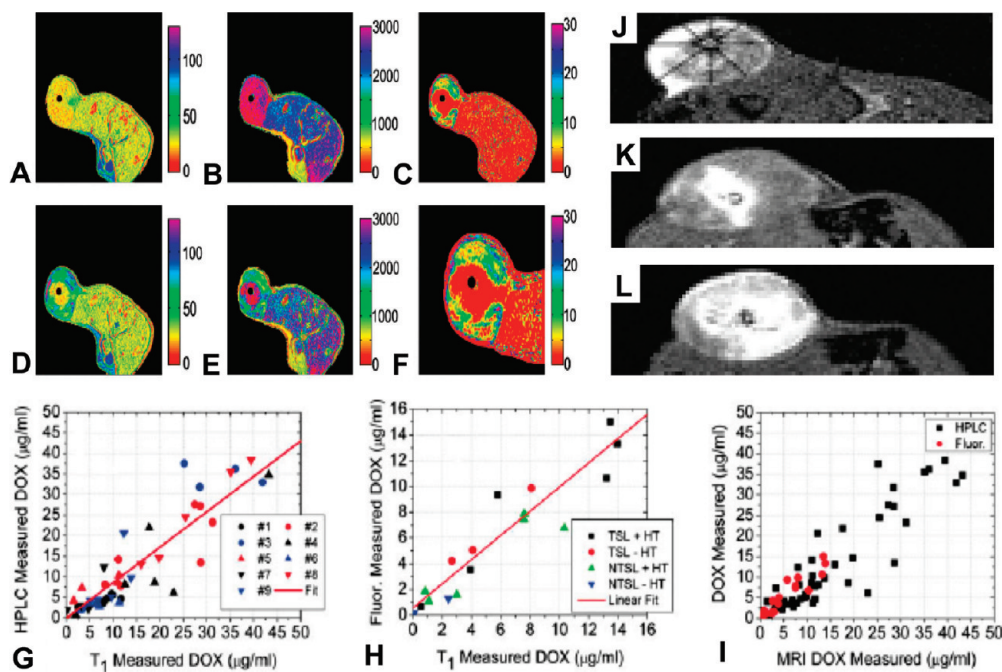


Figure 5. Nanotheranostics for visualizing drug release. A–I: MR-based visualization and quantification of doxorubicin (Dox) release from temperature-sensitive liposomes (TSL) coloaded with MnSO₄ and Dox. A: The initial (i.e., at $t = 0$ min) raw signal intensity map shows an axial view of a rat bearing a flank fibrosarcoma tumor (top left) with a central heating catheter (black spot). B: The initial T_1 intensity map is calculated from a series of multiple flip-angle images. D: The raw signal intensity map at 45 min after the iv injection of TSL in rats bearing preheated fibrosarcoma tumors, exemplifying content release in the periphery of the tumor. E: The calculated T_1 map at 45 min p.i. Note that the regions enhanced in D have reduced T_1 intensity, highlighting contrast agent and drug release through T_1 shortening. C: Dox concentration (in ng/mg tumor) at 45 min p.i., calculated on a pixel-by-pixel basis from the images in panels B and E. F: An enlarged image of panel C, showing the heterogeneity in drug delivery and release (i.e., high in the periphery, low in the center) that can be visualized using this MRI-based methodology. G–I: Procedure for calculating T_1 -based Dox concentrations. Two independent animal experiments demonstrated great agreement between invasive analyses of Dox levels and MRI-based calculations. In G, HPLC was used to quantify Dox concentrations and to correlate them with the results obtained using MRI, and in H, fluorescence measurements were performed. An overlay of both experiments is presented in panel I, exemplifying the precision and the accuracy of MRI for determining Dox levels, even at low concentrations. Images reproduced with permission from ref 29. Copyright 2006 Wiley-Liss, Inc. J–L: Visualization of contrast agent release from TSL coloaded with MnSO₄ and Dox upon the administration of three different regimens of hyperthermia (HT). The enhanced (white) areas represent released manganese. J: TSL administered during steady-state hyperthermia resulted in rapid peripheral enhancement at the edge of the tumor. K: TSL administered before hyperthermia resulted in central enhancement. L: TSL administered in two equal doses, half before hyperthermia and the remainder after steady-state hyperthermia was reached, resulted in uniform enhancement. Reproduced with permission from ref 30. Copyright 2007 The Authors.

TSL to perfuse throughout the tumor toward the central heating source before releasing their contents. Finally, rats were treated with two equal doses of TSL and with a combination of the two above-mentioned heating regimens, and as expected, the first fraction of liposomes released their contents at the center of the tumor, and the second at the periphery, together leading to a very uniform enhancement pattern (Figure 5L). These examples convincingly demonstrate the suitability of this MRI-based methodology to visualize and quantify drug release with high temporal and spatial resolution.^{28–30} Alternative methods to achieve this goal, based for instance on optical (i.e., near-infrared) imaging agents and quenching–dequenching effects, might also enable a real-time visualization of drug release, but no such efforts have been undertaken thus far, and their in vivo

applicability is expected to be limited, due to the limited penetration depth of optical imaging probes and/or to problems associated with quantification.

5. Facilitating Triggered Drug Release. Essentially resulting from three of the above-mentioned applications of nanotheranostics, i.e. visualizing target site accumulation, visualizing drug distribution at the target site and visualizing drug release, is their ability to facilitate triggered drug release. When e.g. not using an invasive catheter to induce hyperthermia in a tumor, but an external heat-producing source, such as in high-intensity focused ultrasound (HIFU), then it would be possible to first visualize the accumulation and the target site distribution of a stimuli-sensitive theranostic nanomedicine formulation, and to then apply radiofrequency waves to those parts of the tumor in which high levels of

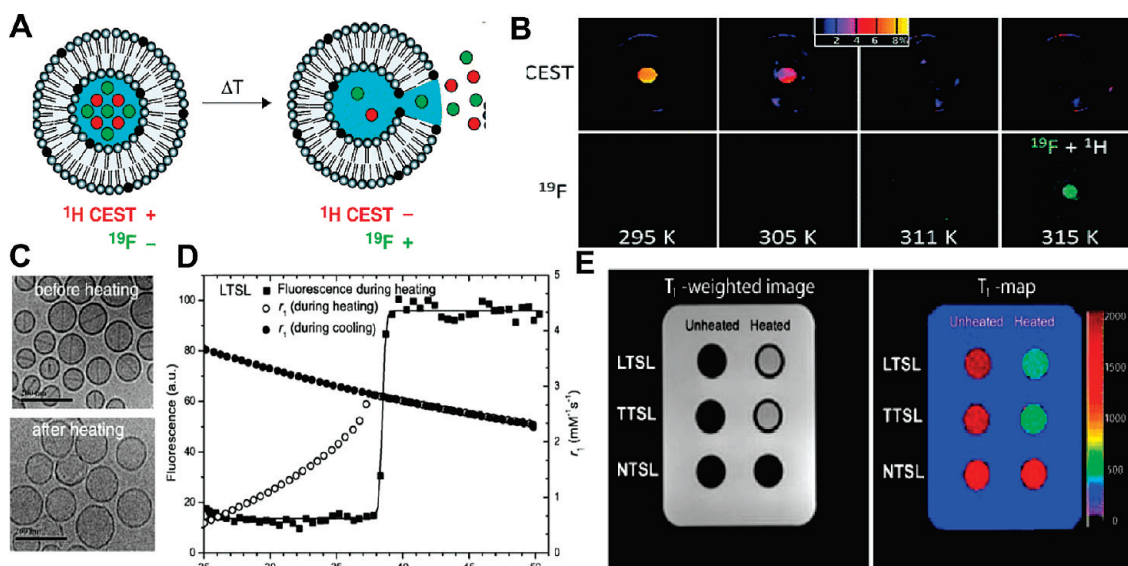


Figure 6. Nanotheranostics for facilitating triggered drug release. A: Generation of a bimodal temperature-sensitive liposomal MR contrast agent which enables the simultaneous visualization of target site accumulation (via a ^1H CEST agent; i.e. $[\text{Tm}(\text{HPDO3A})(\text{H}_2\text{O})]$) and of hyperthermia-induced triggered drug release (via ^{19}F MRI). B: ^1H LipoCEST and ^{19}F MR images of temperature-sensitive liposomes on a clinical 3.0 T MRI scanner. The CEST signal (color scale in percent) vanished at $T \geq 311$ K (i.e., at $T \geq 38$ °C) while the fluorine signal appeared at 315 K (i.e., at $T \geq 42$ °C; overlay with the ^1H image for colocalization and clarity purposes). Images reproduced with permission from ref 31. Copyright 2009 American Chemical Society. C: TEM images of low temperature-sensitive liposomes (LTSL) coloaded with doxorubicin (Dox) and Prohance (i.e., $[\text{Gd}(\text{HPDO3A})(\text{H}_2\text{O})]$) before and after heating to temperatures exceeding the T_g of the LTSL, confirming drug release (i.e., disappearance of the cigar-shaped Dox-crystals). D: Fluorescence and T_1 relaxivity of Dox and Prohance coloaded LTSL during linear temperature increase (0.5 K/min) from 25 to 50 °C. The release of Dox from the aqueous interior of the liposomes was monitored by means of fluorescence, whereas that of coencapsulated Prohance was determined using longitudinal relaxometry (r_1). E: T_1 -weighted images ($\text{TI} = 1500$ ms) and T_1 maps of LTSL, of traditional temperature-sensitive liposomes (TTSL) and of non-temperature-sensitive liposomes (NTSL) before and after heating, exemplifying effective release of Prohance upon hyperthermia. Images reproduced with permission from ref 33. Copyright 2009 Elsevier B.V.

the formulation have accumulated. By doing this, drug release can be triggered not only with high spatial specificity (i.e., in those regions of the target tissue in which high levels of the formulation are present) but also with high temporal specificity (i.e., by applying the trigger at those time points at which the concentration of the formulation at the target site are optimal). To achieve this goal, two different imaging agents need to be incorporated, one which can be visualized while the system is still intact, e.g. a PET tracer or an MR T1 contrast agent with free access to surrounding water molecules (e.g., in case of a liposome: bound to the external bilayer, and not entrapped in the core), and one which does not produce a signal when the system is intact, but only upon release (e.g., an MR T1 contrast agent encapsulated in the

core of a liposome, and shielded from the interaction with surrounding water molecules).

An elegant example of such a theranostic nanomedicine formulation that can be used for facilitating triggered drug release has recently been developed by Langereis, Gruell and colleagues, who have prepared thermosensitive liposomes containing two different MR contrast agents.³¹ This system contains both a CEST agent (i.e., chemical exchange saturation transfer; $[\text{Tm}(\text{HPDO3A})(\text{H}_2\text{O})]$)³² and a ^{19}F probe (i.e., NH_4PF_6), both of which are coloaded into the aqueous interior of the liposomes. At temperatures below the T_g , when the liposomal bilayer is intact and when there is no free access to surrounding water molecules, the CEST agent generates a signal that can be used to track the biodistribution and the target site accumulation of the formulation, and it at the same time quenches the ^{19}F signal (see Figure 6A). Upon heating to temperatures exceeding the T_g , and upon release of both the CEST agent and the ^{19}F probe from the aqueous interior of the liposome, the CEST signal disappears, and the ^{19}F signal appears. Some initial proof-of-principle for the functionality of this system is provided in Figure 6B, which shows that at temperatures ≤ 38 °C, only the CEST signal is observed, while at temperatures ≥ 38 °C, only the fluorine signal is detected.

- (29) Viglianti, B. L.; Ponce, A. M.; Michelich, C. R.; Yu, D.; Abraham, S. A.; Sanders, L.; Yarmolenko, P. S.; Schroeder, T.; MacFall, J. R.; Barboriak, D. P.; Colvin, O. M.; Bally, M. B.; Dewhirst, M. W. Chemodosimetry of in vivo tumor liposomal drug concentration using MRI. *Magn. Reson. Med.* **2006**, *56*, 1011–1018.
- (30) Ponce, A. M.; Viglianti, B. L.; Yu, D.; Yarmolenko, P. S.; Michelich, C. R.; Woo, J.; Bally, M. B.; Dewhirst, M. W. Magnetic resonance imaging of temperature-sensitive liposome release: drug dose painting and antitumor effects. *J. Natl. Cancer Inst.* **2007**, *99*, 53–63.

Using similar temperature-sensitive liposomes, the same group of authors has also set out to develop a theranostic nanomedicine formulation in which doxorubicin is coentrapped with gadolinium in the core of the liposomes.³³ To this end, liposomes containing the MR contrast agent ProHance (i.e., [Gd(HPDO3A)(H₂O)]) and ammonium sulfate were prepared, and doxorubicin was actively postloaded into the liposomes using a pH gradient. Cryo-TEM (transmission electron microscopy) images were obtained for this formulation before and after heating, and as exemplified by Figure 6C, disappearance of the typical cigar-shaped doxorubicin-crystals from the liposomes could be observed upon hyperthermia, thereby confirming drug release. Doxorubicin release was further confirmed by means of fluorescence detection, and this release nicely correlated with the release of ProHance from the liposomes (Figure 6D). It should be noted in this regard that the release of doxorubicin as determined by means of fluorescence detection exhibited a very sharp signal increase at temperatures near the T_g , thereby confirming the excellent suitability of this formulation for hyperthermia-triggered drug release. The increase in the MR signal, on the other hand, was less sharp, but this is due to the fact that the permeability of the liposomal bilayer toward water molecules already starts to increase at temperatures higher than ~ 25 °C. Figure 6E finally shows that the release of the gadolinium-based MR contrast agent upon hyperthermia was only observed for the two temperature-sensitive formulations (i.e., for traditional thermosensitive liposomes (TTS defense) and for low-temperature-sensitive liposomes (LTS defense)), whereas heating did not result in ProHance release from nonthermosensitive liposomes (NTS defense).³³

An added advantage of using such MR-based nanotheranostic formulations for optimizing the efficacy of triggered drug release is that, besides for contrast agent release, MRI can also be used for thermometry. Taking e.g. the above-mentioned strategy into account in which HIFU is used to generate heat specifically in tumorous regions, and to consequently release both drugs and imaging agents from thermosensitive liposomes, it has nowadays become possible to implement innovative HIFU-MRI hardware to simultaneously visualize HIFU-induced temperature increases (using MR thermometry), and the efficiency of triggered drug release (using T1-relaxometry). Clinical studies in which these advanced formulations and hardware tools are being

evaluated are planned for the near future, and the results of these trials are eagerly awaited.

6. Predicting Drug Responses. An additional and clinically highly relevant application of theranostic nanomedicine formulations relates to the use of these systems for predicting therapeutic responses. If, for instance, especially during the initial phases of clinical evaluation, nanomedicines could be labeled with radionuclides or with MR contrast agents, then important noninvasive information could be obtained with regard to target site accumulation, and on the basis of this, rational predictions could be made with regard to the potential effectiveness of the targeted therapeutic interventions to be tested.

In the phase I trial focusing on HPMA copolymer-based doxorubicin (i.e., PK1),³⁴ for instance, a radiolabeled version of this passively tumor-targeted polymeric prodrug (which was termed PK3) could have been used to prescreen patients assigned to PK1, in order to identify which tumors are amenable to EPR-mediated drug targeting and which are not, and to thereby predict which patients are likely to respond to PK1 therapy and which are not.^{35,36} By mixing in trace amounts of PK3 with (e.g., every second cycle of) PK1 during follow-up, and by continuously subjecting patients to 2D-scintigraphy or 3D-PET, it would have furthermore been possible to visualize the efficacy of the intervention in real time (see next section), and consequently to obtain important information for assisting in deciding whether or not to (dis-) continue therapy, and whether or not to adjust drug doses. In this way, nanotheranostics might assist in realizing the potential of “personalized medicine”, i.e. tailor-made therapy for individual patients, which, in addition to the study of genetic polymorphisms and biomarkers, also relies on the development of visual methods for measuring and predicting therapeutic responses.

Some exemplary proof-of-principle for this conceptual advantage of theranostic nanomedicines is provided in Figure 7, which shows the accumulation of radiolabeled PEGylated liposomes in a patient suffering from AIDS-related Kaposi sarcoma, as well as in a patient suffering from severe rheumatoid arthritis. Kaposi sarcomas are characterized by a dense and highly leaky vasculature, and long-circulating and passively tumor-targeted chemotherapeutics efficiently accumulate in these lesions by means of EPR. Consequently, Kaposi sarcoma patients generally respond very well to treatment with PEGylated

- (31) Langereis, S.; Keupp, J.; van Velthoven, J. L.; de Roos, I. H.; Burdinski, D.; Pikkemaat, J. A.; Grüll, H. A temperature-sensitive liposomal 1H CEST and 19F contrast agent for MR image-guided drug delivery. *J. Am. Chem. Soc.* **2009**, *131*, 1380–1381.
- (32) Terreno, E.; Cabella, C.; Carrera, C.; Delli Castelli, D.; Mazzon, R.; Rollet, S.; Stancanello, J.; Visigalli, M.; Aime, S. From Spherical to Osmotically Shrunken Paramagnetic Liposomes: An Improved Generation of LIPOCEST MRI Agents with Highly Shifted Water Protons. *Angew. Chem., Int. Ed.* **2007**, *46*, 966–968.
- (33) De Smet, M.; Langereis, S.; van den Bosch, S.; Grüll, H. Temperature-sensitive liposomes for doxorubicin delivery under MRI guidance. *J. Controlled Release* **2010**, *143*, 120–127.
- (34) Vasey, P. A.; Kaye, S. B.; Morrison, R.; Twelves, C.; Wilson, P.; Duncan, R.; Thomson, A. H.; Murray, L. S.; Hilditch, T. E.; Murray, T.; Burles, S.; Fraier, D.; Frigerio, E.; Cassidy, J. Phase I clinical and pharmacokinetic study of PK1: first member of a new class of chemotherapeutic agents-drug-polymer conjugates. *Clin. Cancer Res.* **1999**, *5*, 83–94.
- (35) Duncan, R. Development of HPMA copolymer-anticancer conjugates: clinical experience and lessons learnt. *Adv. Drug Delivery Rev.* **2009**, *61*, 1131–1148.
- (36) Lammers, T.; Subr, V.; Ulbrich, K.; Hennink, W. E.; Storm, G.; Kiessling, F. Polymeric nanomedicines for image-guided drug delivery and tumor-targeted combination therapy. *Nano Today* **2010**, *5*, 197–212.

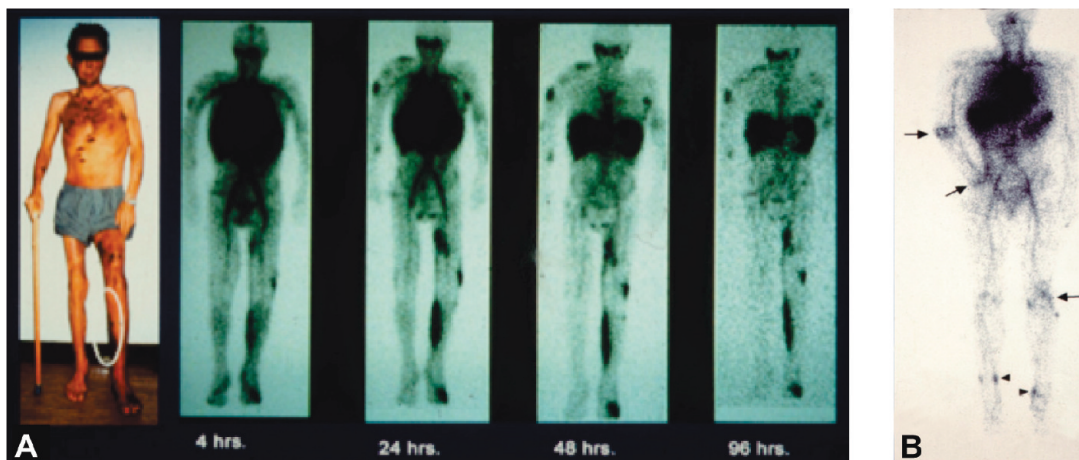


Figure 7. Nanotheranostics for predicting drug responses. A: Biodistribution and tumor accumulation of ^{111}In -labeled PEGylated liposomes in a patient suffering from Kaposi sarcoma. Localization to a large tumorous mass in the lower left leg and to several metastases (e.g., in the upper left leg and in the right shoulder region) can be observed. This high degree of target site localization is in line with the relatively high degree of antitumor activity that can be obtained using PEGylated liposomal doxorubicin (Doxil) in Kaposi sarcoma patients,³⁷ and it exemplifies the possibility of using theranostic nanomedicine formulations to predict treatment responses. Adapted and reprinted with permission from ref 13. Copyright 2001 American Association for Cancer Research. B: Biodistribution and arthritic joint localization of $^{99\text{m}}\text{Tc}$ -labeled PEGylated liposomes in a patient with severe rheumatoid arthritis in the right elbow and wrist, and in the left knee (arrows). Localization to two inflamed soft-tissue infections can also be observed (arrowheads). Also in the case of rheumatoid arthritis, which responds very well to treatment with liposomal and polymeric corticosteroids,^{18–25} theranostic nanomedicines might hold significant potential for predicting drug efficacy. Image courtesy: Dr. Peter Laverman and Prof. Otto Boerman, Dept. of Nuclear Medicine, Radboud University Nijmegen Medical Center, Nijmegen, The Netherlands.

liposomal doxorubicin (i.e., Doxil). In a large phase III trial in which Doxil was compared to the formerly standard combination regimen ABV (i.e., adriamycin (doxorubicin), bleomycin and vincristine), for instance, it was found that Doxil produced 1 complete response and 60 partial responses (in 133 patients; response rate = 46%), compared to only 31 partial responses for ABV (in 125 patients; response rate = 25%).³⁷ This highly significant improvement in therapeutic efficacy can be explained by the fact that Doxil accumulates very well in Kaposi sarcoma lesions, as e.g. in the patient in Figure 7A, whereas in other types of malignancies, its target site accumulation is less effective, and varies substantially from patient to patient. If such patients could be prescreened with radiolabeled Doxil, however, in order to identify which ones show high tumor accumulation and which ones do not, then it would be possible to decide in which cases Doxil treatment should be continued, and in which cases other treatment options should be considered. Analogously, also patients who are to be treated with PEGylated liposomal corticosteroids (to attenuate flares in rheumatoid arthritis; Figure 7B), or patients assigned to antibody-based chemo- or radio-immunotherapy (Figure

3), could be prescreened using such theranostic nanomedicine formulations, in order to discriminate between those showing high and those showing low (or no) target site accumulation, and to thereby predict which patients are likely to respond to such targeted therapeutic interventions and which are not, and to consequently enable optimized and individualized treatment protocols.

7. Evaluating Drug Efficacy Longitudinally. Another important aspect of nanotheranostics and image-guided drug delivery, especially for preclinical purposes, is that they substantially facilitate longitudinal experimental setups, enabling not only more informative and less invasive biodistribution studies but also more elegant and more relevant efficacy analyses, in which e.g. genetically modified mice and orthotopic tumor models are used to study disease progression and treatment outcome in real time. Besides using standard diagnostic procedures, such as MRI with low-molecular-weight gadolinium-based contrast agents or PET with ^{18}F -FDG, to visualize how well non-superficial tumors respond to therapy, likely also gadolinium- or radionuclide-labeled liposomes, polymers, micelles and antibodies hold significant potential for evaluating drug efficacy longitudinally, e.g. by using such theranostic nanomedicines to determine tumor sizes, or by evaluating their ability to accumulate in and visualize metastases (Figure 7A). In addition to this, important information with regard to visualizing the efficacy of the intervention can be obtained by assessing how the target site accumulation of theranostic

(37) Northfelt, D. W.; Dezube, B. J.; Thommes, J. A.; Miller, B. J.; Fischl, M. A.; Friedman-Kien, A.; Kaplan, L. D.; Du Mond, C.; Mamelok, R. D.; Henry, D. H. PEGylated-liposomal doxorubicin versus doxorubicin, bleomycin, and vincristine in the treatment of AIDS-related Kaposi's sarcoma: results of a randomized phase III clinical trial. *J. Clin. Oncol.* **2005**, *16*, 2445–2451.

nanomedicine formulations changes in response to therapy. If, for instance, PEGylated liposomal corticosteroids effectively inhibit local joint inflammation and disease severity in rheumatoid arthritis, then it is likely that their accumulation in these lesions would gradually decrease over time (Figure 7B). By radiolabeling a small fraction of the corticosteroid-containing PEGylated liposomes, their localization to inflamed joints could be visualized noninvasively over time, and since the extent of their target site localization depends on disease severity, it would be possible to use such formulations to track the efficacy of the intervention in real time. Similarly, in the case of actively targeted nanotheranostics, receptor-downregulation and/or the disappearance of receptor-positive pathological cells could be visualized.

An additional interesting application in this regard relates to the use of long-circulating and passively tumor-targeted nanotheranostics for monitoring the efficacy of targeted antiangiogenic interventions. This approach has not yet been evaluated, but some initial proof-of-principle for its potential has already been provided. On the one hand, it has for instance already been demonstrated that by conjugating the highly putative antiangiogenic agent TNP-470 to HPMA copolymers, the balance between the efficacy and the (neuro-) toxicity of this drug can be substantially improved.^{38,39} On the other hand, gadolinium-labeled HPMA copolymers have on various occasions been shown to circulate for prolonged periods of time and, consequently, to hold significant potential for experimental MR angiography.^{40,41} This is exemplified in Figure 8A–D, showing that a 25 kDa-sized gadolinium-containing HPMA copolymer (HE-24.8) can be used to visualize blood vessels in rats and rat tumors with high spatial resolution. Furthermore, as demonstrated in Figure 8E,F, a biodegradable 40 kDa-sized gadolinium-labeled HPMA copolymer (GDCC-40) has been shown to hold potential for visualizing the efficacy of antiangiogenic therapy.⁴² In the latter study, it was found that the VEGF-binding antibody Avastin temporarily inhibited tumor growth and angiogenesis (i.e., between 0 and 36 h after treatment) and that tumors relapsed afterward (i.e., between 36 and 168 h). This biphasic treatment response could be nicely visualized using dynamic contrast-enhanced (DCE-) MRI and

the macromolecular contrast agent GDCC-40, with significant reductions in vascular permeability (K^{trans}) and in the fractional tumor plasma volume (ϕ^{PV}) at 36 h, but with nonsignificant changes compared to pretreatment at 168 h (Figure 8E).⁴² Using a standard low-molecular-weight gadolinium-based contrast agent (i.e., 0.6 kDa-sized Gd-DTPA-BSA; Omniscan), on the other hand, no significant changes were observed during the course of therapy (Figure 8F), exemplifying that the polymer-based MR contrast agent is more suitable for visualizing treatment efficacy longitudinally than is Omniscan. When combining the two above approaches, i.e. the design of a polymer therapeutic carrying TNP-470 and the implementation of a macromolecular MR contrast agent for monitoring antiangiogenic treatment responses, it seems feasible to prepare a long-circulating HPMA copolymer carrying both TNP-470 and gadolinium, and to use this passively tumor-targeted theranostic nanomedicine formulation both for antiangiogenic therapeutic purposes, and for noninvasively visualizing its antivascular and antitumor effects.

8. Combining Disease Diagnosis and Therapy. Combining disease diagnosis and therapy is a final interesting application of nanotheranostics. As the term theranostics is derived from the words diagnostics and therapeutics, it is often the first application that is referred to in this regard. The actual suitability of (nano-) theranostics for disease diagnosis, however, is questionable, especially when disease diagnosis is taken in its strictest sense. On the basis of what, for instance, should the choice for a certain therapeutic agent be based when no proper diagnosis (and staging) has taken place yet? Combining disease diagnosis and therapy should therefore be interpreted in its broadest sense, i.e. with diagnosis not referring to the identification, the localization or the staging of a given pathology, but to the longitudinal monitoring of the therapeutic efficacy of a given drug, or to the prediction of a potential treatment response. Also information with regard to (the balance between) the target site localization and the healthy organ accumulation can be useful from a “diagnostic” point of view, especially in the initial phases of clinical evaluation, as this might enable the early identification of otherwise unexpected side effects. Such applications of theranostic nanomedicine formulations, which bridge the gap between disease diagnosis (in its broadest sense) and therapy, have already been described in the above sections, and they therefore will not be addressed again here.

Conclusions and Future Perspectives

Theranostic nanomedicine formulations can be used for various different purposes. They can be implemented not only to improve disease diagnosis (in its broadest sense; see above) and therapy (by delivering drugs more specifically to the pathological site) but also to facilitate (pre-) clinical efficacy and toxicity analyses, and to better understand various important aspects of the drug delivery process. By enabling a noninvasive assessment of the biodistribution, the target site localization and the target site distribution of pharmacologically active agents, nanotheranostics allows for

-
- (38) Satchi-Fainaro, R.; Puder, M.; Davies, J. W.; Tran, H. T.; Sampson, D. A.; Greene, A. K.; Corfas, G.; Folkman, J. Targeting angiogenesis with a conjugate of HPMA copolymer and TNP-470. *Nat. Med.* **2004**, *10*, 255–261.
- (39) Segal, E.; Satchi-Fainaro, R. Design and development of polymer conjugates as anti-angiogenic agents. *Adv. Drug Delivery Rev.* **2009**, *61*, 1159–1176.
- (40) Kiessling, F.; Heilmann, M.; Lammers, T.; Ulbrich, K.; Subr, V.; Peschke, P.; Waengler, B.; Mier, W.; Schrenk, H. H.; Bock, M.; Schad, L.; Semmler, W. Synthesis and characterization of HE-24.8: a polymeric contrast agent for magnetic resonance angiography. *Bioconjugate Chem.* **2006**, *17*, 42–51.
- (41) Lammers, T.; Subr, V.; Peschke, P.; Kühlein, R.; Hennink, W. E.; Ulbrich, K.; Kiessling, F.; Heilmann, M.; Debus, J.; Huber, P. E.; Storm, G. Image-guided and passively tumour-targeted polymeric nanomedicines for radiochemotherapy. *Br. J. Cancer* **2008**, *99*, 900–910.

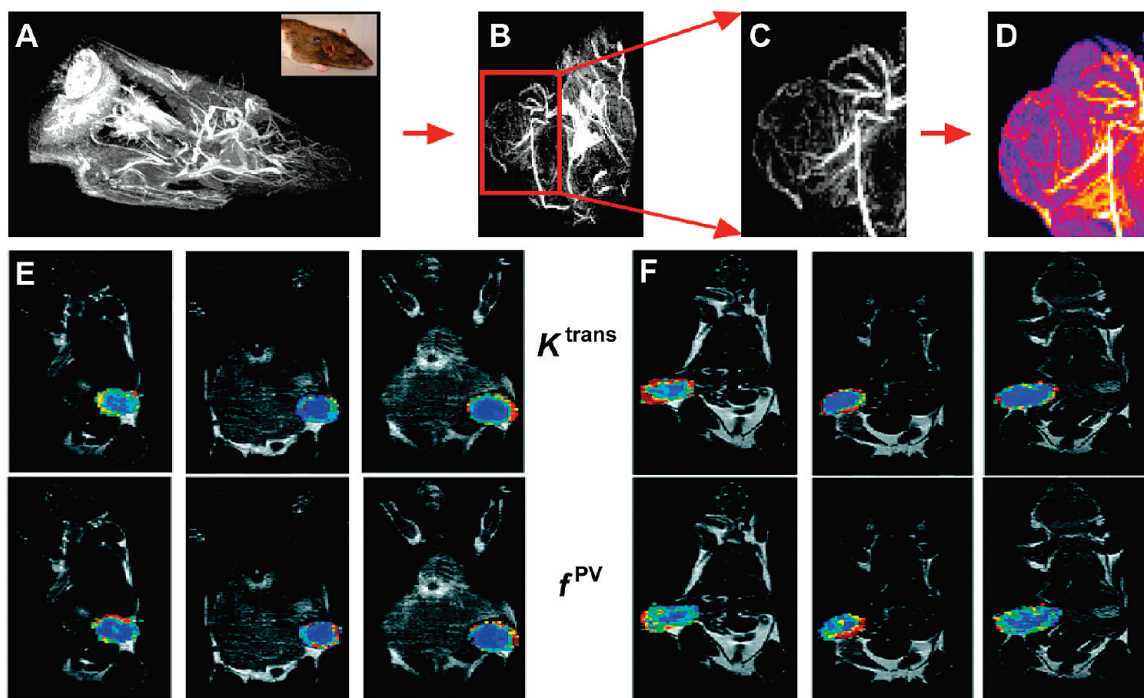


Figure 8. Nanotheranostics for evaluating drug efficacy longitudinally. A–D: MR angiography scans of the chest and head region of a rat (A), of a tumor-bearing paw (B), and of an AT1 tumor (C), obtained at 0.5 h after the iv injection of a 25 kDa-sized gadolinium-labeled HPMA copolymer. Panel D represents a color-coded maximal intensity projection (MIP) of the image in panel C. Such MR angiography-based approaches are considered to be highly suitable for noninvasively visualizing the effect of (antiangiogenic) drug treatment on the structure and function of tumor blood vessels. Images reproduced with permission from ref 41. Copyright 2008 Cancer Research UK. E, F: Representative color-coded K^{trans} (i.e., vascular permeability) and f^{PV} (i.e., fractional plasma volume) maps of tumors in mice before (left panels) and at 36 (middle panels) and 168 (right panels) h after treatment with the antiangiogenic agent Avastin. Dynamic contrast-enhanced (DCE-) MRI was performed using a gadolinium-labeled 40 kDa-sized biodegradable HPMA copolymer (i.e., GDCC-40; panel E) and using a standard low-molecular-weight gadolinium-based contrast agent (i.e., Omniscan; 0.6 kDa; panel F). When determined using GDCC-40, the vascular parameters K^{trans} and f^{PV} correlated significantly better with treatment response than did determinations based on Omniscan. Note that, in this experiment, tumors initially responded relatively well to Avastin treatment (i.e., at 36 h), but later on relapsed (i.e., at 168 h). Images reproduced with permission from ref 42. Copyright 2009 American Chemical Society.

the optimization of drug delivery systems in general, as well as for predicting treatment responses. In addition, by imaging (the kinetics of) drug release *in vivo*, some of the basic properties of drug delivery systems can be visualized and validated, and attempts can be made to correlate the *in vitro* characteristics of drug carriers to their *in vivo* capabilities. Furthermore, by using contrast agents to monitor the release of pharmacologically active agents from nanomedicine formulations, the efficacy of stimuli-sensitive drug delivery systems can be optimized. And finally, by enabling the noninvasive assessment of treatment efficacy *in vivo* in real time, nanotheranostics can be used to facilitate (pre-) clinical efficacy analysis, e.g. in the case of polymer-based passively tumor-targeted antiangiogenic agents.

The clinically most relevant future applications of theranostic nanomedicine formulations relate to their use for optimizing the properties of drug delivery systems, for optimizing the treatment of individual patients, and for better understanding several important aspects of drug targeting to pathological sites. Regarding the former, i.e. the optimization

of the properties of drug delivery systems, the combination of diagnostic and therapeutic agents in a single formulation enables real-time feedback on the biodistribution and the target site accumulation of nanomedicine materials. Various examples of this have been described above (see Figures 2, 3 and 7), and it is clear that by noninvasively visualizing how well drug targeting systems are able to deliver pharmacologically active agents to pathological sites, and how well they are able to prevent these agents from accumulating in potentially endangered healthy tissues (especially those which are highly sensitive to drug exposure), important information can be obtained for optimizing the basic properties of the delivery system, and for improving the balance between the efficacy and the toxicity of such targeted interventions. These insights indicate that theranostic nanomedicine formulations are highly useful not only for optimizing the basic carrier capabilities of drug delivery systems but also for establishing treatment regimens which are able to increase the therapeutic index of systemically administered (chemo-) therapeutic interventions.

By visualizing how well drug targeting systems deliver pharmacologically active agents to the pathological site, and how well they release their contents there, theranostic nanomedicine formulations furthermore facilitate “personalized medicine” and patient individualization, as well as the efficacy of combination regimens. Regarding personalized medicine, it can be reasoned that only in patients which show high levels of target site uptake should treatment be continued, and that in those in which this is not the case, other therapeutic options should be considered. Regarding combination therapies, nanotheranostics enables the temporal and spatial analysis of target site accumulation, and this information could be used to define an optimal timing for combination with other therapeutic modalities. Long-circulating and passively tumor-targeted polymer-based chemotherapeutics, for instance, which were shown to be present in tumorous tissue for prolonged periods of time, combined very well with clinically relevant regimens of fractionated radiotherapy, which was administered on every weekday for several consecutive weeks, and this combination led not only to significant increases in the efficacy of the intervention but also to an improved tolerability^{40,43,44}

Also when intending to use thermosensitive liposomal nanomedicines in conjunction with HIFU-induced hyper-

thermia, image-guidance might be very beneficial. In the case of double-labeled and drug-containing liposomes, it would for instance be possible to noninvasively track the biodistribution and the target accumulation of this formulation (by means of contrast agent nr. 1), to consequently trigger drug release from this formulation at an optimized time point, and to validate the efficacy of HIFU-induced triggered drug release in real time (by means of contrast agent nr. 2). Such approaches and efforts are currently being evaluated within the framework of several cooperative EC-funded integrated projects,^{45–47} and their (chances for) success will besides on the development of appropriate hardware also significantly depend on the generation of suitable theranostic nanomedicine formulations to facilitate their applicability.

In summary, nanotheranostics and image-guided drug delivery can be used for various different purposes, ranging from simple and straightforward biodistribution studies to extensive and elaborate experimental setups aiming to enable “personalized medicine”, and to improve the efficacy of combined modality anticancer therapy. Consequently, we expect that ever more efforts will be invested in developing theranostic nanomedicine formulations, and that these systems and strategies will contribute substantially to realizing the potential of targeted therapeutic interventions.

Acknowledgment. The authors gratefully acknowledge financial support by the European Commission’s Framework Programme 6 (MediTrans: Targeted Delivery of Nanomedicines) and by Hightech.NRW (ForSaTum).

MP100228V

-
- (42) Wu, X.; Jeong, E. K.; Emerson, L.; Hoffman, J.; Parker, D. L.; Lu, Z. R. Noninvasive evaluation of antiangiogenic effect in a mouse tumor model by DCE-MRI with Gd-DTPA cystamine copolymers. *Mol. Pharmaceutics* **2010**, *7*, 41–48.
 - (43) Lammers, T.; Peschke, P.; Kühnlein, R.; Subr, V.; Ulbrich, K.; Debus, J.; Huber, P. E.; Hennink, W. E.; Storm, G. Effect of radiotherapy and hyperthermia on the tumor accumulation of HPMA copolymer-based drug delivery systems. *J. Controlled Release* **2007**, *117*, 333–341.
 - (44) Lammers, T. Improving the efficacy of combined modality anticancer therapy using HPMA copolymer-based nanomedicine formulations. *Adv. Drug Delivery Rev.* **2010**, *62*, 203–231.

- (45) Lammers, T.; Dawson, W.; Storm, G. MEDITRANS: An Integrated Project focusing on targeted nanomedicines sponsored by the European Commission’s Framework Programme. *Drug Discovery*, in press.

- (46) www.meditrans-ip.net.
- (47) www.sonodrugs.eu.